A linear model fails to predict orientation selectivity of cells in the cat visual cortex

M. Volgushev *†‡§, T. R. Vidyasagar *‖ and X. Pei *¶

*Department of Neurobiology, The Max-Planck-Institute for Biophysical Chemistry, Göttingen-Nikolausberg, Germany, †Institute of Higher Nervous Activity and Neurophysiology RAS, Butlerova 5A, Moscow, Russia, ‡Ruhr-Universität Bochum, Medizinische Fakultät, Abteilung für Neurophysiologie, MA 4/149, D-44780 Bochum, Germany, ‖Centre for Visual Science and Division of Neuroscience, John Curtin School of Medical Research, Australian National University, Canberra, ACT 2601, Australia and ¶Department of Physics, University of Missouri at St Louis, 8001 Natural Bridge Road, St Louis, MO 63121, USA

1. Postsynaptic potentials (PSPs) evoked by visual stimulation in simple cells in the cat visual cortex were recorded using *in vivo* whole-cell technique. Responses to small spots of light presented at different positions over the receptive field and responses to elongated bars of different orientations centred on the receptive field were recorded.

2. To test whether a linear model can account for orientation selectivity of cortical neurones, responses to elongated bars were compared with responses predicted by a linear model from the receptive field map obtained from flashing spots.

3. The linear model faithfully predicted the preferred orientation, but not the degree of orientation selectivity or the sharpness of orientation tuning. The ratio of optimal to non-optimal responses was always underestimated by the model.

4. Thus non-linear mechanisms, which can include suppression of non-optimal responses and/or amplification of optimal responses, are involved in the generation of orientation selectivity in the primary visual cortex.

Information processing in the cerebral cortex critically depends on the way excitatory and inhibitory synaptic inputs are summed by single neurones to provide their outputs as action potentials. Debate in this area has focused on the operation of the simple cells of the mammalian visual cortex. One fundamental question has been whether their functional properties, such as orientation, direction and spatial frequency selectivities (Hubel & Wiesel, 1962; Orban, 1984; Henry, Michalski, Wimborne & McCart, 1994), can be adequately explained as the result of a linear summation of their synaptic inputs (Movshon, Thompson & Tolhurst, 1978; Palmer, Jones & Stepnoski, 1991; DeAngelis, Ohzawa & Freeman, 1993), or whether more complicated non-linear processing takes place in the elaborate dendritic tree (Dean, Tolhurst & Wather, 1982; Reid, Soodak & Shapley, 1991; Tolhurst & Dean, 1991). However, these studies have been based on extracellular recordings of action potentials, and thus did not directly address the nature of integration of the subthreshold changes in membrane potential. The introduction of the *in vivo* whole-cell recording technique (Pei, Volgushev, Vidyasagar & Creutzfeldt, 1991) has greatly facilitated the study of postsynaptic potentials (PSPs) evoked by visual stimuli. It has been demonstrated that direction selectivity can be explained by linear mechanisms (Jagadeesh, Wheat & Ferster, 1993). In whole-cell recordings from cat primary visual cortex, we found that the orientation selectivity of the PSP responses to flashed bars could not be predicted from the PSP responses to flashed spots by a linear model. We propose that non-linear summation of PSPs is essential for cortical orientation selectivity.

METHODS

PSPs from neurones in the primary visual cortex of adult cats were recorded using the *in vivo* whole-cell technique described in detail elsewhere (Pei *et al.* 1991; Volgushev, Pei, Vidyasagar & Creutzfeldt, 1993; Pei, Vidyasagar, Volgushev & Creutzfeldt, 1994). Briefly, adult cats bred in the animal house of the Max-Planck-Institute for Biophysical Chemistry in Göttingen were anaesthetized with sodium pentobarbitone (35–40 mg kg^{-1} Nembutal I.P.; Sanofi, Ceva, Germany) or with ketamine hydro-

§ To whom correspondence should be addressed at Ruhr-Universität Bochum, Medizinische Fakultät, Abteilung für Neurophysiologie, MA 4/149, D-44780 Bochum, Germany.

chloride (25 mg kg^{-1} Ketanest LM; Parke-Davis, Berlin). Adequacy of analgesia was tested by squeezing of the toes and pinching of the pinna. During early stages of anaesthesia these noxious stimuli produced retraction of the paw and noticeable changes in heart rate. Surgery was started after these reactions disappeared and stable anaesthesia was achieved. Sometimes this required additional doses of the anaesthetic. After tracheal and venous cannulations and bilateral cervical sympathectomy, the animals were placed in a stereotaxic frame, the skull was exposed and a craniotomy (5 mm diameter) was done over area 17 of the visual cortex centred at P4/L1 (Horsley-Clark). A brass-cylinder (diameter, 20 mm) was cemented over the opening. The hydraulically driven microelectrode holder (David Kopf Instruments, Tujunga, CA, USA) was mounted directly onto the skull with screws and dental cement. All wound edges and pressure points were treated with a local anaesthetic (xylocaine). Muscle relaxation with gallamine triethiodide (Flaxedil; Davis & Geck, Pearl River, NY, USA) and artificial respiration were started either at this point, or earlier during the surgery, when there were indications of respiratory depression which might be due to additional doses of anaesthetics. Thereafter adequate anaesthesia was maintained by I.V. sodium pentobarbitone (1–2 mg kg^{-1} h^{-1}) with a gas mixture of $N_2O:O_2:CO_2$ (70 : 29·2 : 0·8) or with sodium pentobarbitone (3–4 mg kg^{-1} h^{-1}) without nitrous oxide. Wound edges were repeatedly (every 5–8 h) treated with xylocaine. Every 2–3 h adequacy of the anaesthesia was tested by looking for changes in heart rate, blood pressure or EEG while applying noxious stimuli. Any occasional changes such as desynchronized EEG were immediately countered by administering an additional bolus of pentobarbitone (1–2 mg kg^{-1}, I.V.) and by introducing nitrous oxide in the gas mixture in the few instances when the cat was being maintained only on pentobarbitone. Paralysis was maintained by I.V. infusion of gallamine triethiodide (8 mg kg^{-1} h^{-1}) in Ringer solution. Fluid replacement was achieved by the intravenous administration of approximately 4 ml h^{-1} of Ringer solution containing 5% glucose. End-tidal CO_2 was adjusted to 3·5–4·0%; body temperature was maintained around 37–38 °C. Both these parameters were continuously monitored. The EEG was recorded using chlorided silver wires placed on the dura through small skull openings and cemented. Blood pressure was measured regularly using a non-invasive HTC monitor that amplified photoelectrically detected tail pulses. The experiments usually lasted for 2–4 days. At the end of the experiment, the animals were killed with an overdose of sodium pentobarbitone.

The electrodes used were made on a L/M-3P-A puller (List Electronic, Darmstadt, Germany), and filled with a conventional patch pipette solution: 130 mM potassium gluconate, 5 mM NaCl, 10 mM EGTA, 10 mM Hepes, 1 mM ATP, 1 mM $CaCl_2$, 2 mM $MgCl_2$; pH 7·4 (KOH). They had a resistance of 2–7 MΩ. Membrane potentials of recorded cells were −30 to −60 mV, with input resistances of 40–200 MΩ. Visual stimuli were presented on a screen positioned 57 cm in front of the animal, whose eyes were focused on the screen using appropriate contact lenses. The receptive field was first localized with a hand-held projector and then receptive field structure and orientation tuning were investigated with computer-controlled stimuli. Test stimuli were presented for 0·5–1·5 s, with an interval of 1·5–3 s between consequent stimuli. For receptive field plots, we used square light stimuli that were 0·3 deg × 0·3 deg to 1·0 deg × 1·0 deg size. For orientation tuning tests, bars of 0·3–1·0 deg width and 1·5–5 deg length were used. Background illumination was 0·5–1·0 cd m^{-2}. Unattenuated luminance of light stimuli was 30 cd m^{-2}, but stimulus intensity was usually reduced 2–10 times. The matrix for the receptive field plot (usually 5 × 5, 25 pixels, with spot matching the pixel size) was oriented to match the optimal orientation of the cell. For testing orientation tuning, the stimulus was usually centred on the 'on' excitatory zone. We use the terminology of 'on' and 'off' responses to mean PSP changes evoked by turning the light stimulus on and off, respectively. Excitatory responses are depolarizations of the membrane potential and inhibitory responses are hyperpolarizations of the membrane potential. An 'on' region can show either excitation or inhibition, depending on whether depolarization or hyperpolarization was evoked by the stimulus at a certain position. Similarly, an 'off' region can exhibit either excitation or inhibition. Stimuli of different orientations (or locations) were presented in a semi-random order. Receptive fields were classified according to conventional criteria (Orban, 1984). For some cells ordinal position (presence or absence of a monosynaptic thalamic input) was estimated according to the latency of response to electrical stimulation in the lateral geniculate nucleus (Bullier & Henry, 1979). Response strength was estimated as the integral area of averaged PSPs within a window of 20–50 ms that differed from the mean resting membrane potential by more than one standard deviation. We were interested mainly in the early, short latency responses, because these early PSPs are most relevant for studying the origin of orientation selectivity, while later responses can be mostly due to intracortical inputs, which are already orientation selective (Douglas & Martin, 1991; Nelson, Toth, Sheth & Sur, 1994; Douglas, Koch, Machowald, Martin & Suarez, 1995). To minimize the possible influence of intracortical recurrent inputs, a window for measurements was usually positioned over the rising phase of averaged PSP responses, partially covering the peak. In some cells early inhibitory responses could be distinguished and measured with an appropriately positioned window. Since calculated responses usually had longer latencies than measured PSPs, measuring windows were shifted to correct for the latency difference, without changing their width. In some cases spikes were removed by software from individual traces before averaging. The computer algorithm searched for the spikes, then removed them from the beginning to the end, and finally linearly interpolated the continuous signal from the membrane potential before and after the spike. For details of experimental protocol and calculation of predictions of the linear model, see Figs 1 and 2 and the related text.

RESULTS

Our experimental approach is illustrated in Figs 1 and 2. First, we plotted the receptive field with small spots of light, flashed at different positions within a region which covered the receptive field. In the simple first-order cell shown in Fig. 1, EPSPs were evoked by small stimuli (0·5 deg × 0·5 deg) flashed at the central pixels of the matrix (Fig. 1*A*). No significant early responses could be evoked outside this region. The resulting receptive field map of this cell consisted of a single elongated excitatory region (Fig. 1*A*). Second, we recorded the PSPs evoked by flashing bars of different orientations (Fig. 1*B*). The bars were usually centred on the excitatory zone of the receptive field. As quantitative parameters of orientation selectivity, we estimated the selectivity index and tuning width. The orientation selectivity index, k, was calculated as the ratio of the difference between responses to the optimal and non-

optimal orientations divided by their sum:

$$k = (\text{optimal} - \text{non-optimal})/(\text{optimal} + \text{non-optimal}).$$

The selectivity index can vary from 0 (no selectivity) to 1 (maximal selectivity). For evaluation of the tuning width, response amplitudes were plotted against stimulus orientation and the half-width of the curve at half-height was estimated. The responses and parameters of their tuning mentioned so far will be referred to as 'measured'. Third, from the receptive field map we estimated responses of the cell to oriented bars, as predicted in a linear model that assumes that the response to a flashing bar can be obtained from the sum of the responses to individual segments that make up the bar (Fig. 2). Bars of optimal and non-optimal orientations were composed of five pixels positioned along the respective receptive field axis (Fig. 2*A* and *B*). In the more general case, to calculate the predicted response at any given orientation, a bar with the same dimensions as used in the orientation tuning test was projected onto the 5×5 matrix and the measured responses to spots from positions which were covered by the bar were multiplied by corresponding coefficients and summed (Fig. 2*C*). Each coefficient was the portion of the particular pixel of the matrix that was covered by the bar (Fig. 2*C*). Responses to all orientations tested were calculated in this way. Then the orientation selectivity index and tuning width were estimated for these responses. These responses and their tuning will be referred to as 'calculated' or 'predicted'.

The first-order simple cell in Fig. 3 had an elongated receptive field (Fig. 3*A*), and PSP responses evoked in this cell by flashing bars showed marked dependence on stimulus orientation (Fig. 3*B*, continuous lines). Predicted responses (Fig. 3*B*, dashed lines) usually had a longer latency and a different time course than the measured responses. At optimal orientation (Fig. 3*B*, 140 deg), measured responses had almost returned to the baseline after the first EPSP hump, which lasted about 50 ms after the latency, while

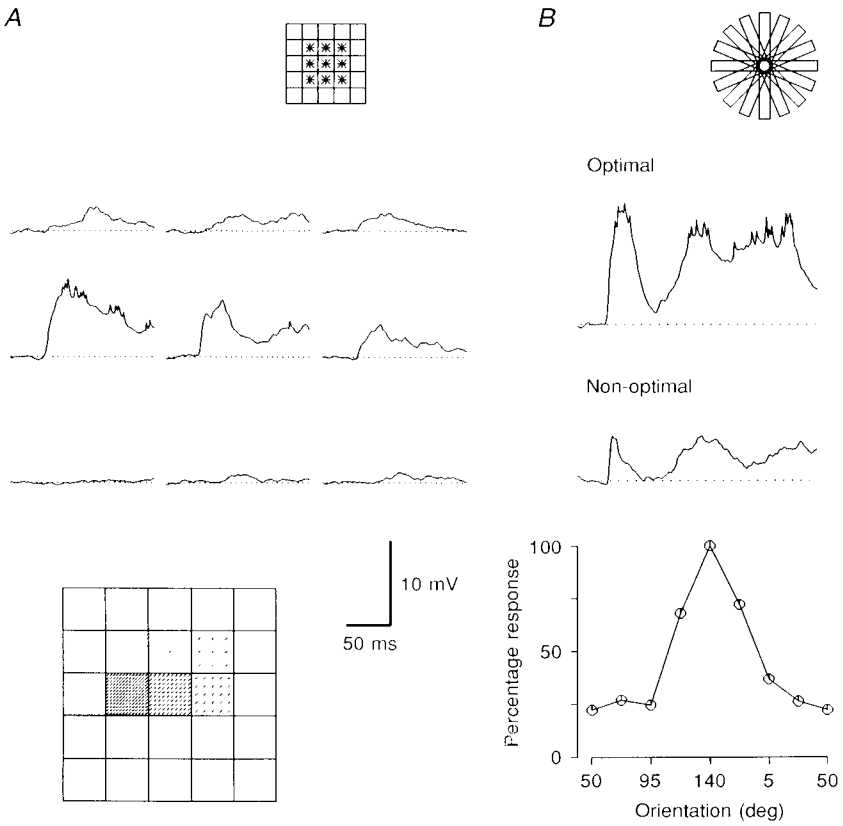

Figure 1. Experimental approach: stimulation protocols

The data are from a first-order simple cell. *A*, receptive field plot. Responses evoked by a spot of light (0·5 deg × 0·5 deg) flashed at each pixel of a 5×5 matrix were recorded. Averaged responses ($n = 5$) evoked from central pixels, marked by asterisks in the inset, are shown. At the bottom is the receptive field map. Response strength is coded by the density of the covering elements. *B*, measurement of orientation tuning. Postsynaptic potentials evoked by a flashed bar (5 deg × 0·4 deg) of different orientations (inset) were recorded. Averaged responses ($n = 5$) to the optimal and non-optimal orientations are shown. Orientation tuning curve for this cell is shown at the bottom. Calibration is common for all traces in *A* and *B*. In this and the following figures, the dotted line shows mean resting membrane potential (−43 mV for this cell); the traces are averages of 5 sweeps and begin with stimulus 'on', unless stated otherwise.

predicted responses stayed well above the baseline. At orientations other than optimal, measured responses had a fast initial rise, and were rapidly attenuated within 5–10 ms after the latency. In contrast, predicted responses did not show clear attenuation and lasted for several tens of milliseconds (Fig. 3*B*). It was typical that both predicted responses and measured PSPs had the same optimal orientation, which corresponded to the long axis of the receptive field. Further, the overall shape of the orientation tuning curve was similar in both cases (Fig. 3*C*). However, calculated responses were less selective than measured PSPs: normalizing the amplitudes of calculated and measured responses to the optimal orientation revealed an almost twofold difference in responses to the non-optimal range of orientations. In accordance, the selectivity index was higher for the measured responses (0·63 *versus* 0·45). Further, the calculated tuning curve is clearly wider than the measured curve (Fig. 3*C*).

The receptive field of the other first-order simple cell consisted of two elongated excitatory and inhibitory regions, positioned one beside the other (Fig. 4*A*). For the orientation tuning test, the bars were centred over the excitatory region. The excitatory region was only mildly elongated, but responses were clearly orientation selective, and the optimal orientation for both measured and calculated responses corresponded to the long receptive field axis (55 deg for this cell; Fig. 4). As in the previous example, responses predicted from the receptive field map were much less selective than measured PSPs. Calculated responses were slightly underestimated (by a factor of 1·4) at the optimal orientation (Fig. 4*B*; 55 deg) and significantly overestimated (by a factor of 3·5) at the non-optimal orientation (Fig. 4*B*; 145 deg). This cell had a clear inhibitory response component, especially pronounced at non-optimal orientations. The inhibitory responses of this cell could be reasonably predicted by the model (Fig. 4*B* and *C*).

In some cells, however, predicted responses differed dramatically from those measured. The first-order simple cell shown in Fig. 5 had only inhibitory 'off' responses to the bar stimuli, but the receptive field exhibited both excitatory and inhibitory regions with small stimuli. In this experiment the stimuli for the orientation tuning test were

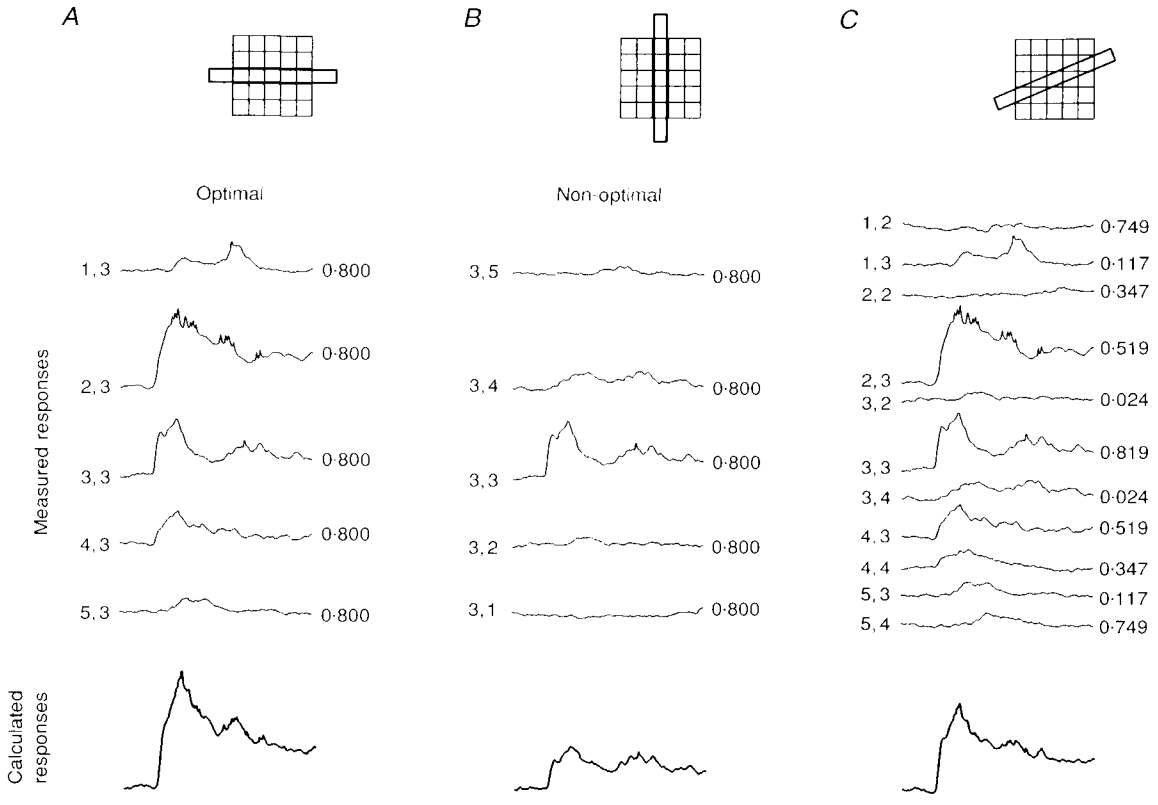

Figure 2. Experimental approach: calculation of the predicted responses

Insets show a bar superimposed on the matrix which was used for the receptive field plot. Responses from the pixels which were covered by the bar are shown, together with their co-ordinates within the matrix (to the left of each trace) and their coefficients, which are portions of the pixel covered by the bar (to the right of each trace). These responses were multiplied by corresponding coefficients and summed to obtain the predicted response, which is shown at the bottom. Optimally and non-optimally oriented bars are composed of only 5 respective pixels each (*A* and *B*). Bars of other orientations are composed of a complex mosaic of parts of many pixels (*C*). The data are from the same cell as in Fig. 1.

centred on the inhibitory zone. Inhibitory responses were clearly underestimated in this cell by a linear model. The measured inhibition was stronger and it could be evoked over a wider range of orientations than was predicted from the receptive field map (Fig. 5*B* and *C*). In contrast, excitatory responses were greatly overestimated. Strong excitation was predicted by the linear model at some orientations, but no significant excitatory responses were recorded at any orientation (Fig. 5*B* and *C*). The most plausible explanation is that inhibition, which was apparent only as moderate membrane hyperpolarization during the receptive field plot, was, however, strong enough to cancel excitatory responses to the bar stimulation.

To compare various parameters of the measured and predicted orientation tuning across the sample, we plotted scatter diagrams, where each cell is represented by an individual point with the abscissa and the ordinate corresponding to the predicted and the measured values, respectively. In the scatter diagram for optimal orientation, all points except one are located on the main diagonal (Fig. 6*A*), which indicates that optimal orientation could be predicted well by a linear model. However, the model could predict neither the selectivity index nor the tuning width. The selectivity index was systematically underestimated: almost all points in Fig. 6*B* are located above the main diagonal, which indicates that predicted values were lower than the actual values. Statistical comparison made for eleven simple cells showed that this difference is highly significant ($P < 0{\cdot}001$; t test value, 3·87). This discrepancy between measured and calculated values arises largely from the overestimation of responses to stimuli of non-optimal orientations. A potential query in our estimation of the selectivity index is the relatively low density of sampling during the receptive field plot. If the receptive field is markedly non-homogeneous within the central pixel (say, occupying only a tiny strip through the pixel centre), which is included in both optimally and non-optimally oriented bars, then in cases when the bar width is less than a single pixel, predicted responses to the optimal orientation could be underestimated. To correct for this potential error,

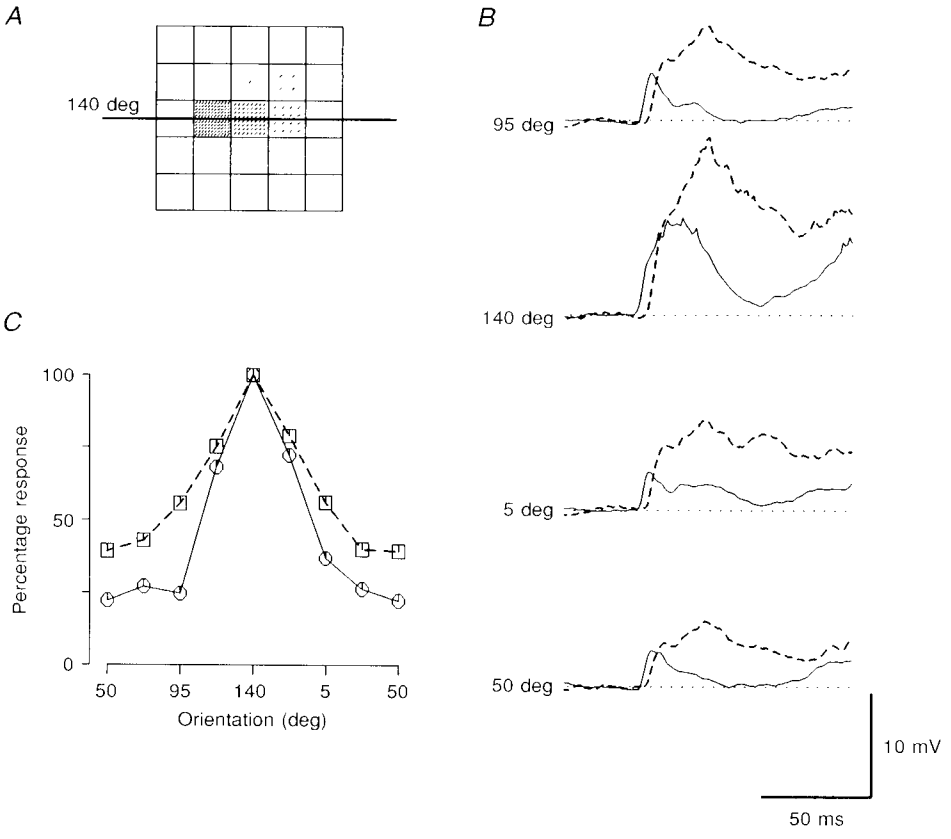

Figure 3. Comparison of measured responses and orientation tuning of a first-order simple cell to the responses and tuning predicted from the receptive field map

A, receptive field map. The test matrix was oriented 140 deg to the horizontal. Response strength is coded by the density of covering. Test stimuli were 0·5 deg × 0·5 deg spots flashed for 1 s. *B*, superposition of measured (continuous line) and predicted (dashed line) responses. Stimulus orientation is indicated at the beginning of each pair of traces. Test stimuli were 5 deg × 0·4 deg bars flashed for 1 s. *C*, orientation tuning curves for measured excitatory responses (○—○) and predicted excitatory responses (□- -□). Measured and predicted tuning curves are scaled to facilitate the comparison.

selectivity indices were recalculated for all those cases (6 out of 11) where bar width was 60–80% of the pixel size. The weight of the central pixel (pixel coefficient; see Fig. 2 and related text) was set to 1 for the optimal orientation. However, this procedure did not change the outcome: recalculated selectivity indices were still lower than the measured ones, and the difference remained highly significant ($P < 0{\cdot}005$; t test value, 3·33).

The tuning width was consistently overestimated by the linear model: most of the points in Fig. 6*C* are located below the main diagonal, indicating that the predicted value was greater than the measured one.

Additional experiments were performed to test whether a linear model overestimates non-optimal responses only in the receptive field centre or in other positions also. Optimally or non-optimally oriented bars were flashed at several positions along the two receptive field axes. The receptive field was also plotted with small spots (as shown in Fig. 1*A*), and responses to the optimal and non-optimal stimuli at the different positions were calculated as explained earlier. The dimensions of the receptive field along both the optimal and non-optimal axes could be well predicted (Fig. 7*A–D*), as has been shown with extracellular recordings. However, the linear prediction overestimated the responses to non-optimal orientations at all locations, leading to an underestimation of the orientation selectivity. This was true even when maximal responses to the optimal and non-optimal orientations were considered irrespective of position: in Fig. 7*E*, most points are above the diagonal.

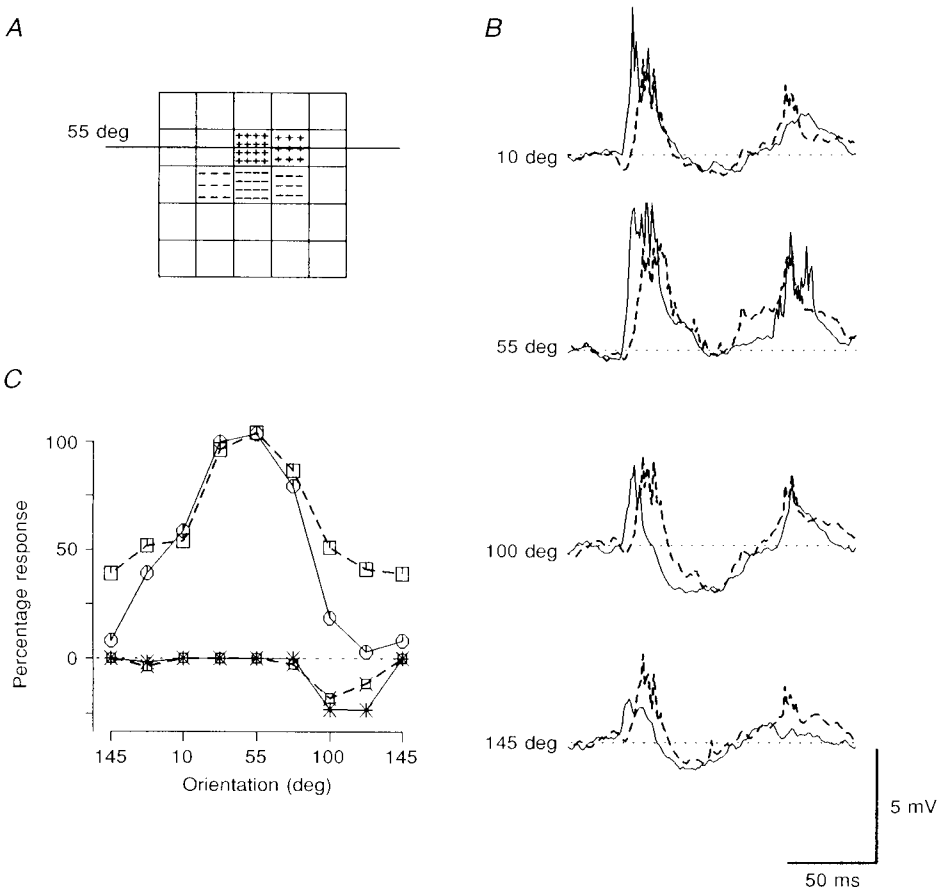

Figure 4. Comparison of measured and predicted responses in a first-order simple cell with a pronounced inhibitory zone in the receptive field

Bars for orientation tuning test were centred on the excitatory zone. *A*, receptive field map. The test matrix was oriented 55 deg to the horizontal. The excitatory zone is shown with plus symbols (+); the inhibitory zone is shown with minus symbols (−). Response strength is coded by the density of the symbols. Test stimuli were 0·5 deg × 0·5 deg spots flashed for 1 s. *B*, superposition of measured (continuous line) and predicted (dashed line) responses. Stimulus orientation is indicated at the beginning of each pair of traces. *C*, orientation tuning curves for measured excitatory responses (○—○), measured inhibitory responses (✳—✳), predicted excitatory responses (□- -□) and predicted inhibitory responses (⌑- -⌑). Stronger inhibitory responses are more negative. Measured and predicted tuning curves for excitatory responses are scaled to facilitate the comparison. Test stimuli were 5 deg × 0·4 deg bars flashed for 1 s.

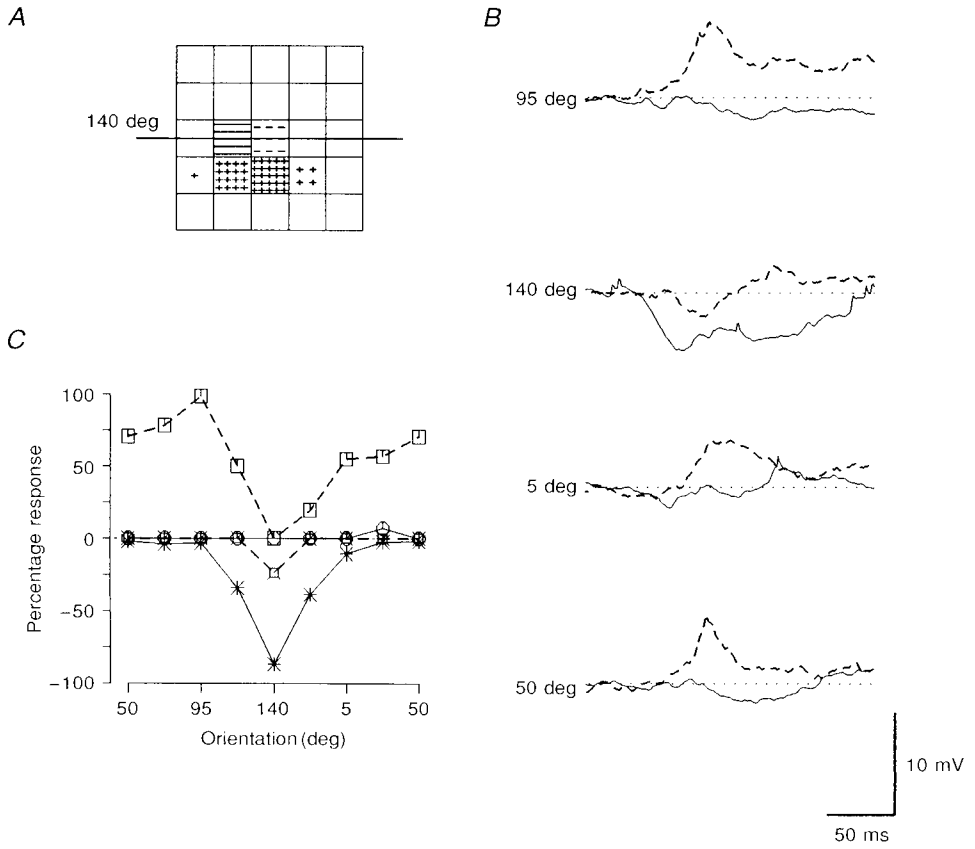

Figure 5. Comparison of measured and predicted responses in a first-order simple cell evoked with bars centred on the inhibitory zone of the receptive field

Conventions as in Fig. 4, but test matrix was oriented 140 deg to the horizontal, 'off' receptive field and responses are shown, and the tuning curves in *C* are not scaled. Test stimuli were 0·5 deg × 0·5 deg spots and 5 deg × 0·4 deg bars.

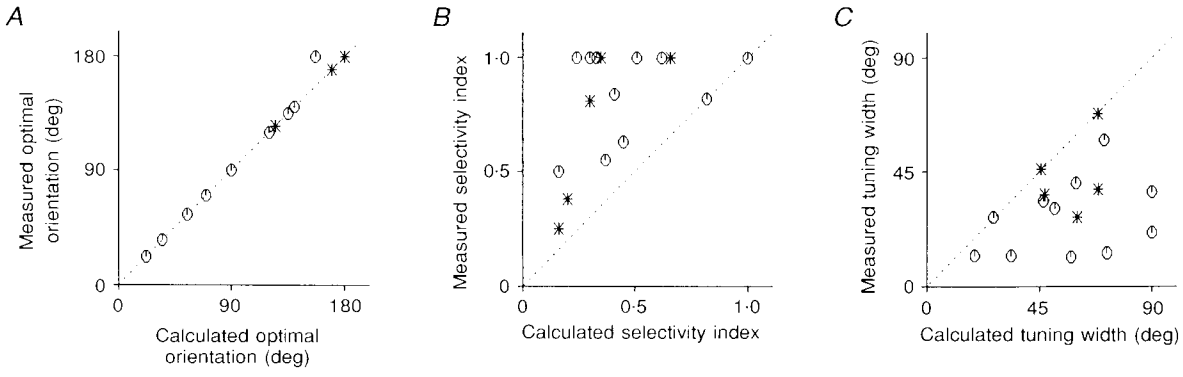

Figure 6. Comparison of parameters of measured and predicted orientation tuning across the sample

Measured values (ordinate) are plotted against values predicted by a linear receptive field model (abscissa). *A*, optimal orientation. *B*, selectivity index, calculated as the difference between optimal and non-optimal responses divided by their sum. *C*, tuning width, calculated as half-width at half-height of the tuning curve. Data for 8 'on' and 3 'off' responses of 9 simple cells (○) are shown. For comparison, data from 2 complex ('on' and 'off' for both) and a simple-like hypercomplex cell are also shown (✳).

DISCUSSION

In our test of spatial summation of visually evoked PSPs in cortical neurones, a linear model of the receptive field failed to predict two aspects of the responses: the shape of individual responses and the sharpness of the orientation tuning.

Predicted responses never matched the measured ones in amplitude and time course. A potential criticism in predicting responses to a bar from the receptive field map obtained with small spots is that the receptive field may not be homogeneous within each single pixel and the response evoked by a stimulus which covers a part of the pixel may not be proportional to the covered area. This could indeed be a problem for prediction of responses to oblique orientations, when a stimulus is composed of complex mosaic of parts of many pixels. But this criticism is not valid for optimal and non-optimal orientations since they correspond to the axes of the matrix used for the receptive field plot. However, the inability of a linear model to predict the shape of individual responses is not necessarily a reflection of non-linearity of spatial summation in the cortex, but could be due to non-linear summation at input cells, for example, to centre–surround antagonism in receptive fields of lateral geniculate neurones. It should also be noted that in some cases calculated responses could be fitted to the recorded PSPs by a combination of linear transformations (shifting along the time axis and amplitude

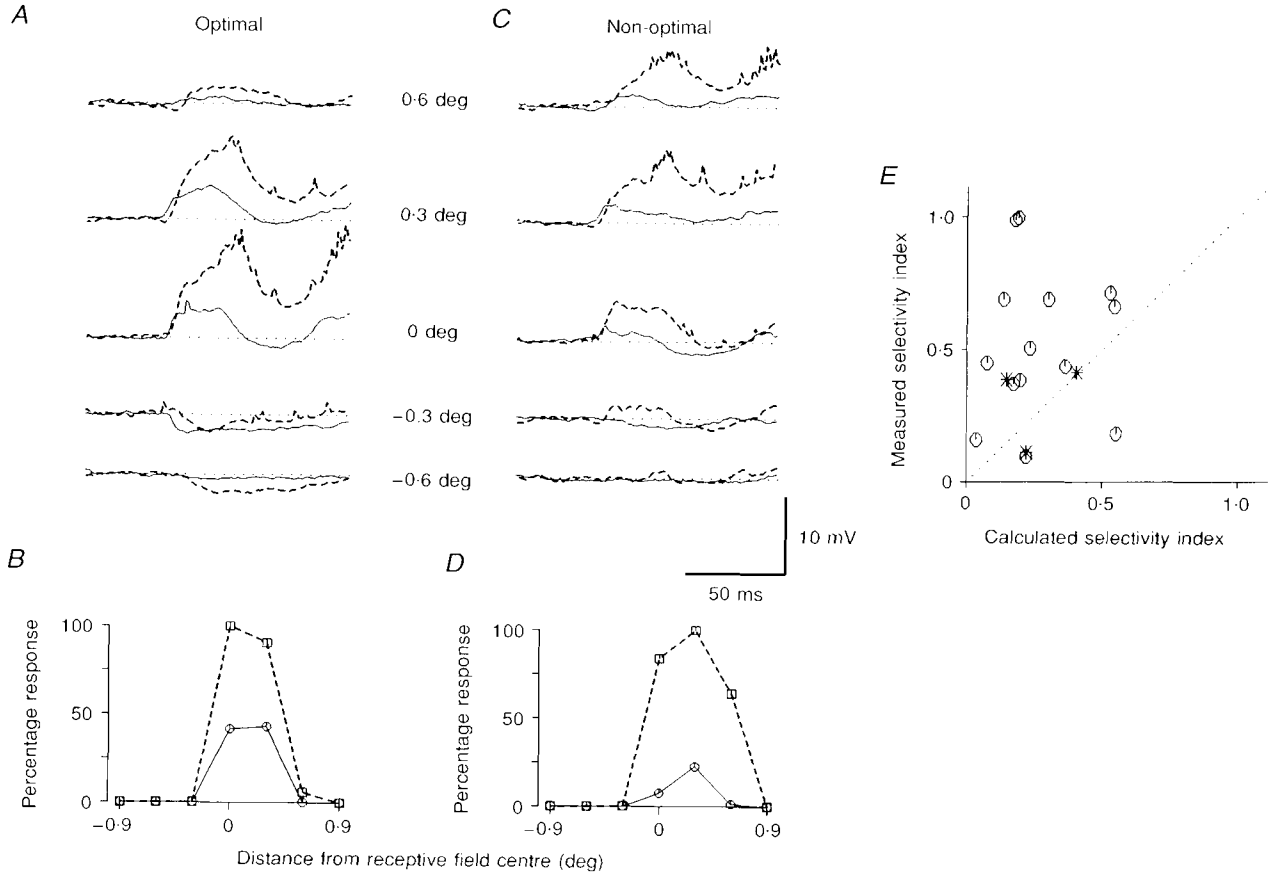

Figure 7. Comparison of measured and predicted responses to bars of optimal and non-optimal orientations at different locations within the receptive field

A and *B* represent responses in the optimum orientation and *C* and *D* in the non-optimum orientation. *A*, averaged (continuous line) and calculated (dashed line) PSP responses of a simple cell to an optimally oriented bar (1·5 deg × 0·3 deg) flashed at different positions. *C*, same as in *A*, but for bars parallel to the non-optimal axis. Location of the test bar relative to the receptive field centre is indicated between *A* and *C*. Receptive field dimensions for bars parallel to the optimal and non-optimal orientations are shown in *B* (optimal) and *D* (non-optimal), respectively. The measured (○–○) and predicted (□- -□) responses along each axis are shown normalized to the maximum response among the two curves. *E*, scatter plot of measured selectivity index against that predicted by the linear receptive field model. Selectivity index was calculated as the difference between maximal responses to optimal and non-optimal orientations divided by their sum. Maximal responses were taken irrespective of the exact position of the stimulus within the receptive field. Data for 8 simple cells (8 'on' and 6 'off' responses, ○), one complex ('on' and 'off' responses, ✳) and one simple-like hypercomplex cell (✳) are shown.

scaling). But predicted responses to different orientations always required different transformations to fit the data. Therefore, the synaptic inputs are summed differently along the optimal and non-optimal axes of the receptive field.

Our data show that a linear model of the receptive field (Hubel & Wiesel, 1962; Ferster, 1986; Chapman, Zahs & Stryker, 1991) could predict only the optimum orientation of a cortical simple cell, but not the degree of selectivity and the sharpness of tuning. The selectivity was consistently underestimated and the tuning width was overestimated. We have recently shown that the excitatory receptive field is only mildly elongated (Pei *et al.* 1994), which might reflect geniculate orientation biases (Vidyasagar & Urbas, 1982) and/or convergence from a slightly elongated row of lateral geniculate receptive fields. The fact that optimum orientation could be consistently predicted in the present experiment indicates that this mild elongation of the excitatory input is indeed crucial in determining the optimum orientation of the cell. However, the final sharp tuning of PSPs, and especially of spike discharges, clearly depends on some additional mechanisms which introduce non-linearity in spatial summation, either by suppressing non-optimal responses and/or by amplifying the optimal. One important factor is intra-cortical inhibition, which might be non-specific (Vidyasagar, 1987; Bonds, 1989), or biased towards the orthogonal orientation (Sillito, 1975; Morrone, Burr & Maffei, 1982; Heggelund & Moors, 1983; Vidyasagar, 1987; Volgushev *et al.* 1993; Pei *et al.* 1994). In either case it would lead to the sharpening of tuning observed in striate cells (Vidyasagar, 1987; Vidyasagar, Pei & Volgushev, 1996). Non-linear effects of inhibition are best illustrated by those cases where the inhibition that was seen only as a weak hyperpolarization was nevertheless able to counteract a strong excitatory drive (Fig. 5). Such non-linearity could have two possible explanations. It could be either due to a shunting inhibition or produced by an inhibitory cell (or cells) with an optimal orientation orthogonal to that of the recorded neurone and requiring length summation for firing. Findings that suppression is often maximal at orientations different from the optimal by 45–90 deg (Heggelund & Moors, 1983; Volgushev *et al.* 1993; Pei *et al.* 1994) and that summation of inhibitory inputs *in vitro* can be highly non-linear (Hirsch, 1995) support this possibility.

A number of mechanisms may contribute to a positive feedback that enhances orientation selectivity (Vidyasagar *et al.* 1996). Optimal responses may be enhanced by voltage-dependent channels that were shown to amplify EPSPs at depolarized membrane potentials *in vitro* (Huguenard, Hamill & Prince, 1989), and might be responsible for increasing the amplitude of visually evoked responses with depolarization *in vivo* (Volgushev, Pei, Vidyasagar & Creutzfeldt, 1992). Intracortical excitatory connections within an orientation column and between iso-orientation columns could further amplify the responses to the optimal orientation (Douglas & Martin, 1991; Nelson *et al.* 1994; Somers, Nelson & Sur, 1995; Douglas *et al.* 1995). The same effect could also be mediated by an excitatory cortico-geniculate circuitry (Sillito, Jones, Gerstein & West, 1994).

Thus, our experiments show that linear models that were successful in predicting direction selectivity (Jagadeesh *et al.* 1993) fail in the case of orientation selectivity. A possible reason for this discrepancy is that tests for direction selectivity have compared responses to moving gratings with those to stationary gratings (or long bars). In the intracellular study of Jagadeesh *et al.* (1993), the stimuli used were different from ours in many respects. They were one-dimensional in the space domain and narrow-band in the temporal frequency domain, while our stimuli were two-dimensional and wide-band in the temporal frequency domain. Further, responses to moving stimuli depend a lot on temporal summation, which is not critical in our experimental situation. There is also the possibility that mechanisms contributing to orientation selectivity may involve non-linearities that may not be apparent when testing directional selectivity to optimally oriented gratings. It would be interesting to test whether the parameters of a linear model that need to be adjusted to predict responses to moving stimuli from responses to stationary stimuli are the same for different orientations.

In conclusion, our direct test of a linear model based on an elongated excitatory receptive field (Hubel & Wiesel, 1962; Ferster, 1986; Chapman *et al.* 1991) showed that only the optimum orientation of a cortical simple cell, but not the degree of orientation selectivity and sharpness of tuning, could be predicted well. We propose that additional mechanisms, such as non-linear suppression of non-optimal responses and/or amplification of optimal responses, are involved in the generation of orientation selectivity in the primary visual cortex.

Bonds, A. B. (1989). Role of inhibition in the specification of orientation selectivity of cells in the cat striate cortex. *Visual Neuroscience* **2**, 41–55.

Bullier, J. & Henry, G. H. (1979). Ordinal position of neurons in the cat striate cortex. *Journal of Neurophysiology* **42**, 1251–1263.

Chapman, B., Zahs, K. R. & Stryker, M. P. (1991). Relation of cortical cell orientation selectivity to alignment of receptive fields of the geniculocortical afferents that arborize within a single orientation column in ferret visual cortex. *Journal of Neuroscience* **11**, 1347–1358.

Dean, A. F., Tolhurst, D. J. & Wather, N. S. (1982). Non-linear temporal summation by simple cells in cat striate cortex demonstrated by failure of superposition. *Experimental Brain Research* **45**, 456–458.

DeAngelis, G. C., Ohzawa, I. & Freeman, R. D. (1993). Spatio-temporal organization of simple-cell receptive fields in the cat's striate cortex. II. Linearity of temporal and spatial summation. *Journal of Neurophysiology* **69**, 1118–1135.

Douglas, R. J., Koch, K., Machowald, M., Martin, K. A. C. & Suarez, H. H. (1995). Recurrent excitation in cortical circuits. *Science* **269**, 981–985.

Douglas, R. J. & Martin, K. A. C. (1991). A functional microcircuit for cat visual cortex. *Journal of Physiology* **440**, 735–769.

Ferster, D. (1986). Orientation selectivity of synaptic potentials in neurones of cat primary visual cortex. *Journal of Neuroscience* **6**, 1284–1301.

Heggelund, P. & Moors, J. (1983). Orientation selectivity and the spatial distribution of enhancement and suppression in receptive fields of cat striate cortex cells. *Experimental Brain Research* **52**, 235–247.

Henry, G. H., Michalski, A., Wimborne, B. M. & McCart, R. J. (1994). The nature and origin of orientation specificity in neurons of the visual pathways. *Progress in Neurobiology* **43**, 381–437.

Hirsch, J. A. (1995). Synaptic integration in layer IV of the ferret striate cortex. *Journal of Physiology* **483**, 183–199.

Hubel, D. & Wiesel, T. N. (1962). Receptive fields, binocular interaction and functional architecture in the cat's visual cortex. *Journal of Physiology* **160**, 106–154.

Huguenard, J. R., Hamill, O. P. & Prince, D. A. (1989). Sodium channels in dendrites of rat cortical pyramidal neurons. *Proceedings of the National Academy of Sciences of the USA* **86**, 2473–2477.

Jagadeesh, B., Wheat, H. S. & Ferster, D. (1993). Linearity of summation of synaptic potentials underlying direction selectivity in simple cells of the cat visual cortex. *Science* **262**, 1901–1904.

Morrone, M. C., Burr, D. C. & Maffei, L. (1982). Functional implications of cross-orientation inhibition of cortical visual cells. I. Neurophysiological evidence. *Proceedings of the Royal Society* B **216**, 335–354.

Movshon, J. A., Thompson, I. D. & Tolhurst, D. J. (1978). Spatial summation in the receptive fields of simple cells in the cat's striate cortex. *Journal of Physiology* **283**, 53–77.

Nelson, S., Toth, L., Sheth, B. & Sur, M. (1994). Orientation selectivity of cortical neurons during intracellular blockade of inhibition. *Science* **265**, 774–777.

Orban, G. A. (1984). *Neuronal Operations in the Visual Cortex*. Springer-Verlag, Berlin.

Palmer, L. A., Jones, J. P. & Stepnoski, R. A. (1991). Striate receptive fields as linear filters: characterization in two dimensions of space. In *Vision and Visual Dysfunction*, vol. 4, ed. Cronley-Dillon, J., pp. 246–265. Macmillan Press, London.

Pei, X., Vidyasagar, T. R., Volgushev, M. & Creutzfeldt, O. D. (1994). Receptive field analysis and orientation selectivity of postsynaptic potentials of simple cells in cat visual cortex. *Journal of Neuroscience* **14**, 7130–7140.

Pei, X., Volgushev, M., Vidyasagar, T. R. & Creutzfeldt, O. D. (1991). Whole-cell recording and conductance measurements in cat visual cortex *in vivo*. *NeuroReport* **2**, 485–488.

Reid, R. C., Soodak, R. E. & Shapley, R. M. (1991). Directional selectivity and spatiotemporal structure of receptive fields of simple cells in cat visual cortex. *Journal of Neurophysiology* **66**, 505–529.

Sillito, A. M. (1975). The contribution of inhibitory mechanisms to the receptive field properties of neurons in the striate cortex of the cat. *Journal of Physiology* **250**, 305–329.

Sillito, A. M., Jones, H. E., Gerstein, G. L. & West, D. C. (1994). Feature-linked synchronization of thalamic relay cell firing induced by feedback from the visual cortex. *Nature* **369**, 479–482.

Somers, D. C., Nelson, S. B. & Sur, M. (1995). An emergent model of orientation selectivity in cat cortical simple cells. *Journal of Neuroscience* **15**, 5448–5465.

Tolhurst, D. J. & Dean, A. F. (1991). Evaluation of a linear model of directional selectivity in simple cells of the cat's striate cortex. *Visual Neuroscience* **6**, 421–428.

Vidyasagar, T. R. (1987). A model of striate response properties based on geniculate anisotropies. *Biological Cybernetics* **57**, 11–23.

Vidyasagar, T. R., Pei, X. & Volgushev, M. (1996). Multiple mechanisms underlying the orientation selectivity of visual cortical neurones. *Trends in Neurosciences* **19**, 272–277.

Vidyasagar, T. R. & Urbas, J. V. (1982). Orientation sensitivity of cat LGN neurones with and without inputs from visual cortical areas 17 and 18. *Experimental Brain Research* **46**, 157–169.

Volgushev, M., Pei, X., Vidyasagar, T. R. & Creutzfeldt, O. D. (1992). Postsynaptic potentials in the cat visual cortex: dependence on polarization. *NeuroReport* **3**, 679–682.

Volgushev, M., Pei, X., Vidyasagar, T. R. & Creutzfeldt, O. D. (1993). Excitation and inhibition in orientation selectivity of cat visual cortex neurons revealed by whole-cell recordings *in vivo*. *Visual Neuroscience* **10**, 1151–1155.

Acknowledgements

We are deeply indebted to Professor Otto D. Creutzfeldt for his support of this project and active participation in many of the experiments. However, since this paper was prepared after his death, we did not feel that it would be legitimate to include his name despite his many valuable contributions. We are grateful to Drs A. Kreiter, S. Löwel, M. Munk and G. Henry for critically reading the manuscript. M.V. was supported by the Alexander von Humboldt Foundation and by the Max Planck Society.

Author's email address

M. Volgushev: maxim@neurop.ruhr-uni-bochum.de

Received 31 January 1996; accepted 22 July 1996.